Phylogenetic Analysis of SARS-CoV-2 Genomes in Turkey

Ogün ADEBALİ*, Aylin BİRCAN, Defne ÇİRCİ, Burak İŞLEK, Zeynep KILINÇ, Berkay SELÇUK, Berk TURHAN

Molecular Biology, Genetics and Bioengineering, Faculty of Natural Sciences and Engineering, Sabancı University, İstanbul, Turkey

***Correspondence:** oadebali@sabanciuniv.edu

ORCIDs:

Ogun Adebali: https://orcid.org/0000-0001-9213-4070

Aylin Bircan: https://orcid.org/0000-0001-6663-6173

Defne Çirci: https://orcid.org/0000-0002-5761-0198

Burak İşlek: https://orcid.org/0000-0003-2700-9884

Zeynep Kılınç: https://orcid.org/0000-0002-1906-0391

Berkay Selçuk: https://orcid.org/0000-0003-3206-4749

Berk Turhan: https://orcid.org/0000-0002-6471-0357

Phylogenetic Analysis of SARS-CoV-2 Genomes in Turkey

Abstract: COVID-19 has effectively spread worldwide. As of May 2020, Turkey is among the top ten countries with the most cases. A comprehensive genomic characterization of the virus isolates in Turkey is yet to be carried out. Here, we built a phylogenetic tree with 15,277 severe acute respiratory syndrome coronavirus 2 (SARS-CoV-2) genomes. We identified the subtypes based on the phylogenetic clustering in comparison with the previously annotated classifications. We performed a phylogenetic analysis of the first thirty SARS-CoV-2 genomes isolated and sequenced in Turkey. Our results suggest that the first introduction of the virus to the country is earlier than the first reported case of infection. Virus genomes isolated from Turkey are dispersed among most types in the phylogenetic tree. Two of the seventeen sub-clusters were found enriched with the isolates of Turkey, which likely have spread expansively in the country. Finally, we traced virus genomes based on their phylogenetic placements. This analysis suggested multiple independent international introductions of the virus and revealed a hub for the inland transmission. We released a web application to track the global and interprovincial virus spread of the isolates from Turkey in comparison to thousands of genomes worldwide.

Keywords: SARS-CoV-2, COVID-19, phylogenetics, evolution, genome sequence

1. Introduction

Severe acute respiratory syndrome coronavirus 2 (SARS-CoV-2) has emerged in Wuhan (Li, et al. 2020) and spread across continents and eventually resulted in the COVID-19 pandemic. Although there are significant differences between the current and ancestral SARS-CoV genome, the reason behind it's pandemic behaviour is still unclear. Genome sequences around the world were revealed and deposited into public databases such as GISAID (Shu and McCauley 2017). It is crucial to reveal the evolutionary events of SARS-CoV-2 to understand the types of the circulating genomes as well as in which parts of the genome differ across these types.

The SARS-CoV-2 virus originated from SARS-CoV, and the intermediate versions between two human viruses were found in bats and pangolins (Li, et al. 2020). The virus has been under a strong purifying selection (Li, et al. 2020). With the genomes obtained so far, the sequences of SARS-CoV-2 genomes showed more than 99.9% percent identity suggesting a recent shift to the human species (Tang, et al. 2020). Still, there are clear evolutionary clusters in the genome pool. Various studies use different methods such as SNP based (Tang, et al. 2020) or entropy (Zhao, et al. 2020) based to identify evolving virus strains to reveal genomic regions responsible for transmission and evolution of the virus. Tang et. al identified S and L strains among 103 SARS-CoV-2 genomes based on two SNPs at ORF1ab and ORF8 regions which encode replicase/transcriptase and ATF6, respectively (Tang, et al. 2020). Entropy-based approach generated informative subtype markers from 17 informative positions to cluster evolving virus genomes (Zhao, et al. 2020). Another study defined a competitive subtype based on D614G mutation at spike

protein which is facilitates binding to ACE2 to receptor on the host cell surface (Bhattacharyya, et al. 2020).

In this work, we used publicly available SARS-CoV-2 genome datasets. We aligned the whole genome sequences of more than 15,000 genomes and built a phylogenetic tree with the maximum likelihood method. We clustered the genomes based on their clade distribution in the phylogenetic tree. The genome characteristics are identified and associated with the previous studies. We further analysed clusters, mutation and transmission patterns of the genomes from Turkey.

2. Materials and methods

To perform our analyses we retrieved virus genomes, aligned them to each other and revealed the evolutionary relationships between them through phylogenetic trees. We assigned the clusters based on the mutations for each genome. We further analyzed the phylogenetic tree with respect to neighbor samples of our genomes of interest to identify possibly transmission patterns.

2.1. Data retrieval, multiple sequence alignment and phylogenomic tree generation

The entire SARS-CoV-2 genome sequences, along with their metadata were retrieved from the GISAID database **(Table-S1)** (Shu and McCauley 2017). We retrieved the initial batch of genomes (3,228) from GISAID on 02/04/2020. We used Augur toolkit to align whole genome sequences using mafft algorithm (--reorder --anysymbol –nomemsave). The SARS-CoV2 isolate Wuhan-Hu-1 genome (GenBank:NC_045512.2) is used as a reference genome to trim the sequence and remove insertions in the

genomes. Since the initial batch, the new sequences in GISAID were periodically added to the pre-existing multiple sequence alignment (--existing-alignment). The final multiple sequence alignment (MSA) contained 15,501 genomes that were available on May 1st 2020. In the metadata file, some genomes lacked month and day information and only had the year of the sample collection date. The genomes with incomplete information were filtered out and the unfiltered MSA consisted of 15,277 sequences. Maximum likelihood phylogenetic tree was built with IQ-TREE with the following options: -nt AUTO (on a 112-core server) -m GTR -fast. Augur was used to estimate the molecular clock through TimeTree (Sagulenko, et al. 2018). For Figure 2, IQ-TREE multicore version 1.6.1 was used for the construction of the maximum likelihood tree. Ultra-fast bootstrapping option is used with 1000 bootstraps for the transition genome tree.

The sub-tree consisting of Turkey isolates were retrieved from the master time-resolved tree with the 'Pruning' method from ete3 toolkit (Huerta-Cepas, et al. 2016). The tree is visualized in FigTree v1.4.4 (http://tree.bio.ed.ac.uk/software/figtree/), and rerooted by selecting EPI_ISL_428718 as an outgroup. The branch lengths of EPI-ISL-417413 and EPI-ISL-428713 samples are shortened for better visualization. ggtree (Yu, et al. 2017) package in R was used to generate the tree and corresponding clusters.

2.2. Genome clustering

We generated phylo-clusters with TreeCluster (Balaban, et al. 2019) which is specifically designed to group viral genomes. The tool supports different clustering

options and we used the default option which is called as "Max Clade". Max Clade finds clusters based on two parameters. The first one is the "-t" option, which defines the threshold that two leaf nodes can be distant from each other. The second option "-s" is used to assign a minimum support value that connects two leaf nodes or clades. For our analysis, we only used the distance threshold. Max Clade algorithm requires leaves to form a clade and satisfy the distance threshold at the same time.

We tried different thresholds until the convergence to the clusters that we obtained. We decided on the number of phylo-clusters and phylo-subgroups based on their similarity with different clusters that are previously reported (see below). We used -t parameter as 0.0084 and 0.00463 for phylo-clusters and phylo-subclusters, respectively. After retrieving the groupings from TreeCluster, we eliminated clusters containing less than 100 sequences (except one sub-cluster that contains 99 sequences). We classified those clusters having less than 100 sequences as not clustered. As a result, we obtained four primary and 17 sub-clusters.

L/S clustering was performed by considering the nucleotides at 8782nd and 28144th positions. In case nucleotides in these positions forms "TC" haplotype, the sequence is categorized as S type. Sequences whose nucleotide combination at the specified positions is "CT" , categorized as L type .In case both these positions correspond to a gap, the sequence is classified as N type. All other cases are categorized as unknown type. 614 G/D clustering applied based on the amino acid at the 614th position of the spike protein (Jaimes, et al. 2020). Combinations of the nucleotides at positions 241;1059; 3037; 8782; 11083; 14408; 14805; 17747; 17858; 18060; 23403; 25563; 26144; 28144; 28881; 28882; 28883 determined the subtypes for barcode clustering.

Sequences that belong to the ten major subtypes (with more than 100 sequences) which constitute %86 percent of all sequences were labelled with their respective 17 nucleotide combination (Zhao, et al. 2020). All other sequences were classified as unknown for barcode classification. Six major clusters (Morais Júnior, et al. 2020) were assigned by the previously determined twelve positions (3037; 8782; 11083; 14408; 17747; 17858; 18060; 23403; 28144; 28881; 28882; 28883). Nucleotide combinations in these positions formed six major subtypes; the rest was categorized as unknown. The lineages were assigned using the proposed nomenclature by Rabaut et al. through Pangolin COVID-19 Lineage Assigner web server (Rambaut, et al. 2020).

2.3. Distance calculations

We rooted the maximum-likelihood tree for distance calculations by selecting samples that belong to bats and pangolin as an outgroup, namely EPI-ISL-412976, EPI-ISL-412977, and EPI-ISL-412860. We measured the distance from leaf to root for every leaf node that is present in the phylogenetic tree with the ete3 toolkit (Huerta-Cepas, et al. 2016).

2.4. Variant information processing

Mutations for each position in the multiple sequence alignment, were mapped into a table relative to the reference genome (GenBank:NC_045512.2) with a custom script. A table of all the mutations of only selected sequences was created and ordered according to the phylogenetic tree of the selected sequences. Mutations that do not correspond to a nucleotide such as a gap or N were labeled as “Gap or N”; the other mutations were marked as Nongap. For variations that do not correspond to gap or N, respective

nucleotides in the reference genome were taken and added to the table to retrieve the associated substitution information. The GFF file of the reference genome (GCF_009858895.2) was extracted from NCBI's Genome database (NCBI). Open reading frame (ORF) information of each mutation was retrieved through the GFF file and added to the table. Positions that are not in the range of any ORF were labelled as "Non-coding region". Codon information and position of each mutation in the reference genome were retrieved according to their respective ORF start positions and frame. In this process, reported frameshifts in ORF1ab and ORF7a and 7b were taken into account. Coding information was used to assign amino acid substitution information to the variations. Amino acid substitution information was used to categorize variants as non-synonymous, synonymous, non-coding regions.

2.5. Migration analysis

The maximum-likelihood phylodynamic analysis was performed with Treetime (Sagulenko, et al. 2018) to estimate likely times of whole-genome sequences of SARS-CoV-2 by computing confidence intervals of node dates and reconstruct phylogenetic tree into the time-resolved tree. The slope of the root-to-tip regression was set to 0.0008 to avoid inaccurate inferences of substitution rates. With this model, we eliminated the variation of rapid changes in clock rates by integration along branches (standard deviation of the fixed clock rate estimate was set to 0.0004). The coalescent likelihood was performed with the Skyline (Strimmer and Pybus 2001) model to optimize branch lengths and dates of ancestral nodes and infer the evolutionary history of population size. The marginal maximum likelihood assignment was used to assign internal nodes to their most likely dates. Clock rates were filtered by removing tips that deviate more than

four interquartile ranges from the root-to-tip versus time regression. JC69 model was used as General time-reversible (GTR) substitution models to calculate transition probability matrix, actual substitution rate matrix, and equilibrium frequencies of given attributes of sequences. The distribution of subleading migration states and entropies were recorded for each location through Augur trait module (sampling bias correction was set to 2.5). Closest child-parent pairs that do not go beyond their given locations were identified and evaluated as transmissions using Auspice (Hadfield, et al. 2018).

3. Results

3.1. Phylogenetic map of the virus subtypes

The first COVID-19 case in Turkey was reported on March 10^{th,} 2020, later than the reported first incidents in Asian and European countries. Since then, the number of cases increased massively. We used all the genomes available in the GISAID database as of May 1^{st,} 2020 and built a phylogenetic tree. After we filtered out the samples with a lack of information, the total number of samples we eventually used was 15,277. The phylogenetic tree was built with the maximum likelihood method and a time-resolved tree was generated **(Figure 1)**. To verify the accuracy of the phylogenetic tree as well as to assess the distribution of well-characterized genomic features, we mapped several classification schemes on the tree; (i) S/L strain type(Tang, et al. 2020); (ii) D614G type(Bhattacharyya, et al. 2020); (iii) barcodes(Zhao, et al. 2020); (iv) six major clusters. Although the methodologies of the clustering attempts were different between these studies, in general, the previously established groups were in line with our phylogenetic tree. Besides the already established clustering methods, we classified the clades based on the phylogenetic tree only. There are two levels of clustering, as we

termed phylo-clusters and phylo-subclusters. Small clusters were not taken into account (see Methods). The phylogenetic map of the virus genomes clearly shows the two major S and L strain clades. As the ancestral clade, S-strain is seen as limited in the number of genomes. 29 of the 30 isolates in Turkey are classified in the L-type group.

The samples from Turkey are dispersed throughout the phylogenetic tree **(Figure 1)**. The 30 samples are classified in 3 out of 4 different phylo-clusters and one is remained unclassified. This dispersion suggest multiple independent introductions to the country. 7 of the 30 genomes have aspartic acid (D) at the 614th position of the Spike protein. The rest 23 genomes have glycine (G) in the same position. Although it was claimed that D614G mutation is becoming dominant because it enables smoother transmission of the virus (Bhattacharyya, et al. 2020) this correlation might simply be the founder effect which is basically the loss or gain of a genetic information when large population arise from a single individual.

3.2. A transient genome between S and L strain suggests early introduction

One of the genomes isolated in Turkey (EPI-ISL-428718) clustered together with the early subtypes of the virus. This genome contains T at the position 8782, which is a characteristic of the S-strain; however, it has T at the position 28144, which implies the L-strain. Therefore, this sample is characterized as neither S-strain nor L-strain by their footprints. In the phylogenetic tree, this genome is placed between S and L strains, which suggests a transitioning genome from S to L strain **(Figure 2).** The number of variant nucleotides between this sample and root is lower than the other Turkey samples. Phylogenetic placement in the earliest cluster, which is closer to the root,

suggests that the lineage of EPI-ISL-428718 entered Turkey as one of the first genomes. By the time this sample was isolated in Turkey, the L-strain had started to spread in Europe, primarily in Italy. Although the isolation date of this early sample is one week later than the first reported case, the existence of an ancestral genome sequence suggests an earlier introduction of SARS-CoV-2 to Turkey.

3.3. Cluster profiles of the samples

Turkey has genome samples from at least three of the four major clusters. By taking the transitioning genome into account, samples of Turkey are genuinely scattered in the phylogenetic tree. Based on the groupings applied, we analyzed the distribution of the clusters in Turkey and other countries **(Figure 3A)**. The most samples of Turkey belong to cluster 3. Iran, Denmark and France are also enriched in cluster 3. Unlike China, South Korea, Spain and the USA, cluster 1 (S-strain) sample has not been observed in Turkey yet. Most European countries are enriched in cluster 3. Although Turkey has cluster 3 genomes, the fraction of them is lower compared to those countries. With the available genome sequences, the overall cluster profile of Turkey seems to be unique. The divergence of the samples from to tree root was calculated for each sub-cluster. The sub-clusters observed in Turkey were analyzed only along with the other countries **(Figure 3B)**. The divergence rates are comparable in general. However, within the same sub-clusters, virus genomes collected in Turkey have averagely more diverged than their relatives in other countries. The isolated genomes assigned to sub-cluster 4 and 8 show higher divergence rates in Turkey compared to the others in the same cluster (p-value: 0.00001 and 0.006, respectively). This observation possibly suggests either or both of the two scenarios; (i) the viruses dominantly circulating in Turkey were

introduced to the country later than other countries or (ii) this sub-cluster has been circulating in Turkey at a relatively higher rate than other countries and diverged more.

3.4. Mutation analysis of the genomes retrieved in Turkey

We used 30 Turkey isolates to analyze their mutational patterns and corresponding clusters further. From the master tree, we pruned all the leaves except for the samples of interest. We rooted the subtree at the transition sample. We aligned the assigned clusters and all the mutations relative to the reference genome **(Figure 4),** illustrating a correlation between the mutation pattern and the phylogenetic tree clades. Observation of no recurrence of a mutation suggests many mutations have resulted in a founder effect in the analyzed samples.

In total, 55 unique mutations were detected, 2 and 20 of which are non-coding and synonymous. Thirty-three unique amino acid substitutions are detected (Table 2). D614G mutation is claimed to be more aggressive because of its easier transmission. A recent report also showed that viruses with 614G genotype results in higher fatality rates (Becerra-Flores and Cardozo 2020). 23 out of 30 genomes we analyzed have 614G mutation. D614G mutation seems to have mutated with the two synonymous mutations in ORF1ab **(Figure 4)**. Besides 614G, three more amino acid substitutions were identified in the spike protein **(Table 2)**. G206A, T951I, G227S, S911F, A1420V, A3995F mutations in ORF1a and V772I, T1238I mutations in Spike protein, V66L in ORF5 and S54L in ORF8 are found specific to some isolates in Turkey **(Table 2)**. The most abundant amino acid substitutions (23/30) are P314L (ORF1b) and D614G (Spike), which are not enriched in Turkey and dispersed worldwide. ORF1a V378I and

ORF9 S194L are found in 7 and 6 of the 30 isolates, respectively, and show high fraction (15 folds with respect to general) in Turkey.

The mutational landscape represents the natural classifications of major and sub-clusters. These mutational footprints can be used to identify the clusters of the future genomes.

3.5. Trace of the spread

Based on the number of mutations we observe since December 2019, SARS-CoV-2 genome mutates twice a month, on average. As genome sequencing reveals mutations, it enables a better understanding of the epidemiology by identifying patterns of virus transmission. The time-resolved phylogenetic distributions of the genomes collected in Turkey suggested at least three sources of introduction **(Figure 5A)**. The earliest introduction seems to be originated from the US. The second international movement observed was from Australia. The third and latest introduction of the virus is from Europe, mostly based in the UK. There is a connection between Saudi Arabia and the two cities in Turkey. Based on the model, this association is reciprocal. The Europe-based introductions are seen as the genomes isolated in Istanbul. Within Turkey, the transmission hub appears to be Ankara **(Figure 5B)**. The isolates in 5 cities are associated with a virus isolated in Ankara **(Figure 5C).**

3.6. Web application to trace virus transmission

We have published a web application powered by Auspice (sarscov2.adebalilab.org/latest). We employed the front-end package (Auspice) that

283 Nextstrain uses (Hadfield, et al. 2018). With increasing number of virus strains, not far
284 from now, it will be infeasible to display the entire phylogenetic tree even in modern
285 browsers. Nextstrain handles this problem by grouping the datasets based on the
286 continents. As the aim of this platform is to trace the spread of virus genomes associated
287 with Turkey, we will use representatives in the phylogenetic tree. The representative
288 sequences will cover all the subtypes. The genomes of the samples collected in Turkey
289 and their nearby sequences will be kept. With this approach, the web application will
290 always contain the genome data from Turkey and necessary information of the subtypes
291 with the representative sequences. An additional dimension we added to the application
292 is that it enables to trace virus across the cities of Turkey. This approach is applicable to
293 create a comprehensive platform for migration analysis for any country or region of
294 choice.
295

296 **4. Discussion**

297 There are two most abundant lineages of isolates in Turkey: sub-clusters 4 and 8. If the
298 30 samples unbiasedly represent the overall distribution of the strains in Turkey, sub-
299 clusters 4 and 8 might comprise approximately 80% of the genomes in the country. More
300 genomes should be sequenced and analyzed to gain more insight into virus evolution. It
301 is essential to continuously follow up on the upcoming mutations when new samples are
302 added to GISAID database.
303

304 The phylogenetic analysis of the circulating genomes in a country is necessary to identify
305 the specific groups and their unique mutational patterns. The success of the COVID-19
306 diagnosis test kits, antibody tests and protein-targeting drugs possibly depend on the

variation of the genomes. If a mutation affects protein recognition, the sensitivity of the test might drastically reduce. Therefore, mutation profiles of the isolates abundantly circulating in the country should be taken into account towards these aims. As international travels are limited, the genome profiles of the countries differ from each other. If international transmissions are kept being restricted, distinct cluster profiles might establish. Therefore, each country might need to develop their specific tests targeting the abundant genomes circulating in local.

The spread of the virus is traced by the personal declarations and travel history of the infected people. As SARS-CoV-2 genomes spread, they leave foot prints behind (mutations) allowing us to trace them. It is feasible to complement the conventional approach with genome sequencing in an unbiased way. Implemented feature of city-based tracing of the virus should be useful for authorities to take necessary measures to prevent spread. This approach will be automated in a standard pipeline. We aim to eliminate the technical limitations (because of the size) by applying filtering methods without losing any relevant information.

Acknowledgments

This work, in part, is supported by the European Molecular Biology Organization (EMBO) Installation Grant (OA) funded by The Scientific and Technological Research Council of Turkey (TÜBİTAK). OA is additionally supported by International Fellowship for Outstanding Researchers Program, TÜBİTAK 2232 and BAGEP (Young Scientist Award by Science Academy, Turkey) 2019 grant. DÇ, ZK and BT are supported by the TÜBİTAK STAR program 2247-C.

We would like to thank all the healthcare workers who save lives during the COVID-19 pandemic. We thank the research groups who made the genome datasets available for accelerating research. So far, three groups in Turkey submitted genome sequences; 26 genomes were provided by the Ministry of Health (Fatma Bayrakdar, Ayşe Başak Altaş, Yasemin Coşgun, Gülay Korukluoğlu, Selçuk Kılıç); 3 submitted by the GLAB (Ilker Karacan, Tugba Kizilboga Akgun, Bugra Agaoglu, Gizem Alkurt, Jale Yildiz, Betsi Köse, Elifnaz Çelik, Mehtap Aydın, Levent Doganay, Gizem Dinler); 1 submitted by Erciyes University (Shaikh Terkis Islam Pavel, Hazel Yetiskin, Gunsu Aydin, Can Holyavkin, Muhammet Ali Uygut, Zehra B Dursun, İlhami Celik, Alper Iseri, Aykut Ozdarendeli).

We thank Dr. Barış Süzek for his helpful comments on the manuscript. We would like to acknowledge Cem Azgari for his contributions throughout the project. We thank Molecular Biology Association for their leadership in taking the initiative of forming a pool of volunteers in COVID-19 testing. Finally, we would like to thank the members of Ecology and Evolutionary Biology Association in Turkey for fruitful discussions regarding the preliminary analysis of the SARS-CoV-2 genomes.

Authors' contribution

OA conceived the study, designed the analysis, interpreted the results and wrote the first draft. AB generated the multiple sequence alignments, Bİ generated the visualization pipeline with auspice. BS generated the clusters based on the phylogenetic tree and plotted cluster graphs. DÇ, ZK and BT assigned previously identified clusters to the

355 genomes, visualized the clusters aligned with the tree and identified mutations per
356 sample. All authors contributed to manuscript writing and revising.
357
358 **References**
359 Balaban M, Moshiri N, Mai U, Jia X, Mirarab S (2019). TreeCluster: Clustering
360 biological sequences using phylogenetic trees. PLoS One 14:e0221068
361 Becerra-Flores M, Cardozo T (2020). SARS-CoV-2 viral spike G614 mutation exhibits
362 higher case fatality rate. Int J Clin Pract
363 Bhattacharyya C, Das C, Ghosh A, Singh AK, Mukherjee S, Majumder PP, Basu A,
364 Biswas NK (2020). Global Spread of SARS-CoV-2 Subtype with Spike Protein Mutation
365 D614G is Shaped by Human Genomic Variations that Regulate Expression of
366 TMPRSS2 and MX1 Genes. bioRxiv 2020.2005.2004.075911
367 Hadfield J, Megill C, Bell SM, Huddleston J, Potter B, Callender C, Sagulenko P, Bedford
368 T, Neher RA (2018). Nextstrain: real-time tracking of pathogen evolution. Bioinformatics
369 34:4121-4123
370 Huerta-Cepas J, Serra F, Bork P (2016). ETE 3: Reconstruction, Analysis, and
371 Visualization of Phylogenomic Data. Mol Biol Evol 33:1635-1638
372 Jaimes JA, Andre NM, Chappie JS, Millet JK, Whittaker GR (2020). Phylogenetic
373 Analysis and Structural Modeling of SARS-CoV-2 Spike Protein Reveals an
374 Evolutionary Distinct and Proteolytically Sensitive Activation Loop. J Mol Biol
375 Li C, Yang Y, Ren L (2020). Genetic evolution analysis of 2019 novel coronavirus and
376 coronavirus from other species. Infect Genet Evol 82:104285
377 Li Q, Guan X, Wu P, Wang X, Zhou L, Tong Y, Ren R, Leung KSM, Lau EHY, Wong
378 JY, Xing X, Xiang N, Wu Y, Li C, Chen Q, Li D, Liu T, Zhao J, Liu M, Tu W, Chen C,

379 Jin L, Yang R, Wang Q, Zhou S, Wang R, Liu H, Luo Y, Liu Y, Shao G, Li H, Tao Z,
380 Yang Y, Deng Z, Liu B, Ma Z, Zhang Y, Shi G, Lam TTY, Wu JT, Gao GF, Cowling BJ,
381 Yang B, Leung GM, Feng Z (2020). Early Transmission Dynamics in Wuhan, China, of
382 Novel Coronavirus-Infected Pneumonia. N Engl J Med 382:1199-1207
383 Li X, Giorgi EE, Marichann MH, Foley B, Xiao C, Kong X-P, Chen Y, Korber B, Gao F
384 (2020). Emergence of SARS-CoV-2 through Recombination and Strong Purifying
385 Selection. bioRxiv 2020.2003.2020.000885
386 Morais Júnior IJ, Polveiro RC, Souza GM, Bortolin DI, Sassaki FT, Lima ATM (2020).
387 The global population of SARS-CoV-2 is composed of six major subtypes. bioRxiv
388 2020.2004.2014.040782
389 Rambaut A, Holmes EC, Hill V, O'Toole Á, McCrone J, Ruis C, du Plessis L, Pybus OG
390 (2020). A dynamic nomenclature proposal for SARS-CoV-2 to assist genomic
391 epidemiology. bioRxiv 2020.2004.2017.046086
392 Sagulenko P, Puller V, Neher RA (2018). TreeTime: Maximum-likelihood phylodynamic
393 analysis. Virus Evol 4:vex042
394 Shu Y, McCauley J (2017). GISAID: Global initiative on sharing all influenza data - from
395 vision to reality. Euro Surveill 22:
396 Shu Y, McCauley J (2017). GISAID: Global initiative on sharing all influenza data–from
397 vision to reality. Eurosurveillance 22:
398 Strimmer K, Pybus OG (2001). Exploring the demographic history of DNA sequences
399 using the generalized skyline plot. Mol Biol Evol 18:2298-2305
400 Tang X, Wu C, Li X, Song Y, Yao X, Wu X, Duan Y, Zhang H, Wang Y, Qian Z, Cui J,
401 Lu J (2020). On the origin and continuing evolution of SARS-CoV-2. National Science
402 Review

403 Yu G, Smith DK, Zhu H, Guan Y, Lam TT-Y (2017). ggtree: an r package for
404 visualization and annotation of phylogenetic trees with their covariates and other
405 associated data. Methods in Ecology and Evolution 8:28-36
406 Zhao Z, Sokhansanj BA, Rosen GL (2020). Characterizing geographical and temporal
407 dynamics of novel coronavirus SARS-CoV-2 using informative subtype markers.
408 bioRxiv 2020.2004.2007.030759

409

410 **Table 1 - The genome sequences identified in Turkey.** See the Supplementary Table
411 – S1 for the full list. All authors are listed in the acknowledgments in detail. GLAB is
412 the Genomic Laboratory that is a conjoint lab of Health Directorate of Istanbul and
413 Istanbul Technical University. The genomes are sorted by the sample collection date.

Accession	Date	City	Lab	Authors
EPI_ISL_429866	3/16/20	Afyon	Ministry of Health Turkey	Bayrakdar et al.
EPI_ISL_417413	3/17/20	Ankara	Ministry of Health Turkey	Bayrakdar et al.
EPI_ISL_424366	3/17/20	Kayseri	Erciyes University	Pavel et al.
EPI_ISL_428712	3/17/20	Karaman	Ministry of Health Turkey	Bayrakdar et al.
EPI_ISL_429867	3/17/20	Balikesir	Ministry of Health Turkey	Bayrakdar et al.
EPI_ISL_429868	3/17/20	Eskisehir	Ministry of Health Turkey	Bayrakdar et al.
EPI_ISL_429869	3/17/20	Konya	Ministry of Health Turkey	Bayrakdar et al.
EPI_ISL_428716	3/18/20	Ankara	Ministry of Health Turkey	Bayrakdar et al.
EPI_ISL_428713	3/18/20	Ankara	Ministry of Health Turkey	Bayrakdar et al.
EPI_ISL_428715	3/18/20	Nevşehir	Ministry of Health Turkey	Bayrakdar et al.
EPI_ISL_428714	3/18/20	Kastamonu	Ministry of Health Turkey	Bayrakdar et al.
EPI_ISL_429865	3/18/20	Çanakkale	Ministry of Health Turkey	Bayrakdar et al.
EPI_ISL_428717	3/19/20	Kocaeli	Ministry of Health Turkey	Bayrakdar et al.
EPI_ISL_428718	3/19/20	Kocaeli	Ministry of Health Turkey	Bayrakdar et al.
EPI_ISL_428719	3/21/20	Siirt	Ministry of Health Turkey	Bayrakdar et al.
EPI_ISL_428720	3/21/20	Ankara	Ministry of Health Turkey	Bayrakdar et al.
EPI_ISL_428721	3/21/20	Ankara	Ministry of Health Turkey	Bayrakdar et al.
EPI_ISL_428722	3/22/20	Balıkesir	Ministry of Health Turkey	Bayrakdar et al.
EPI_ISL_428723	3/22/20	Aksaray	Ministry of Health Turkey	Bayrakdar et al.
EPI_ISL_429870	3/22/20	Sakarya	Ministry of Health Turkey	Bayrakdar et al.
EPI_ISL_429861	3/22/20	Ankara	Ministry of Health Turkey	Bayrakdar et al.
EPI_ISL_429862	3/22/20	Ankara	Ministry of Health Turkey	Bayrakdar et al.
EPI_ISL_429863	3/22/20	Sakarya	Ministry of Health Turkey	Bayrakdar et al.
EPI_ISL_429864	3/22/20	Sakarya	Ministry of Health Turkey	Bayrakdar et al.
EPI_ISL_429871	3/23/20	Ankara	Ministry of Health Turkey	Bayrakdar et al.
EPI_ISL_429873	3/23/20	Kocaeli	Ministry of Health Turkey	Bayrakdar et al.
EPI_ISL_429872	3/25/20	Kocaeli	Ministry of Health Turkey	Bayrakdar et al.
EPI_ISL_427391	4/13/20	İstanbul	GLAB	Karacan et al.
EPI_ISL_428368	4/16/20	İstanbul	GLAB	Karacan et al.
EPI_ISL_428346	4/17/20	İstanbul	GLAB	Karacan et al.

414 **Table 2 - Amino acid substitutions observed in 30 samples.** The amino acid
415 substitutions observed in Turkey are listed. The number of the overall substitutions were
416 retrieved from CoV-GLUE database. The total number of genomes in the database was
417 inferred from the D614G substitution which we found to be 63% of all the genomes.
418 The substitutions that are observed at least in two isolates with enrichment factor greater
419 than 2 are marked. (nt: nucleotide; aa: amino acid; EF: enrichment factor; sub:
420 substitution)
421
422

nt pos	nt sub	aa pos	aa sub	ORF	CoV-GLUE	Turkey (30)	CoV-GLUE fraction	Turkey fraction	EF	
881	G > A	206	A>T	ORF1a	2	2	0.00	0.07	565.60	*
884	C > T	207	R>C	ORF1a	52	4	0.00	0.13	43.51	*
944	G > A	227	G>S	ORF1a	1	1	0.00	0.03	565.60	
1397	G > A	378	V>I	ORF1a	206	7	0.01	0.23	19.22	*
1437	C > T	391	S>F	ORF1a	27	1	0.00	0.03	20.95	
2997	C > T	911	S>F	ORF1a	1	1	0.00	0.03	565.60	
3117	C > T	951	T>I	ORF1a	1	2	0.00	0.07	1131.19	*
4524	C > T	1420	A>V	ORF1a	1	1	0.00	0.03	565.60	
8371	G > T	2702	Q>H	ORF1a	22	1	0.00	0.03	25.71	
8653	G > T	2796	M>I	ORF1a	55	4	0.00	0.13	41.13	*
11083	G > T	3606	L>F	ORF1a	2222	8	0.13	0.27	2.04	*
12248	G > T	3995	A>S	ORF1a	1	1	0.00	0.03	565.60	
12741	C > T	4159	T>I	ORF1a	4	2	0.00	0.07	282.80	*
12809	C > T	4182	L>F	ORF1a	3606	1	0.21	0.03	0.16	
14122	G > T	219	G>C	ORF1b	3	1	0.00	0.03	188.53	
14408	C > T	314	P>L	ORF1b	10651	23	0.63	0.77	1.22	
17690	C > T	1408	S>L	ORF1b	36	3	0.00	0.10	47.13	*
21304	C > A	2613	R>N	ORF1b	5	1	0.00	0.03	113.12	
21305	G > A	2613	R>N	ORF1b	5	1	0.00	0.03	113.12	
21452	G > T	2662	G>V	ORF1b	2662	1	0.16	0.03	0.21	
23403	A > G	614	D>G	ORF2	10691	23	0.63	0.77	1.22	
23599	T > A	679	N>K	ORF2	2	1	0.00	0.03	282.80	
23876	G > A	772	V>I	ORF2	1	1	0.00	0.03	565.60	
25275	C > T	1238	T>I	ORF2	1	1	0.00	0.03	565.60	
25563	G > T	57	Q>H	ORF3	4131	18	0.24	0.60	2.46	*
26718	G > T	66	V>L	ORF5	2	2	0.00	0.07	565.60	*
28054	C > T	54	S>L	ORF8	1	1	0.00	0.03	565.60	
28109	G > T	72	Q>H	ORF8	72	2	0.00	0.07	15.71	
28854	C > T	194	S>L	ORF9	220	6	0.01	0.20	15.43	*
28878	G > A	202	S>N	ORF9	66	1	0.00	0.03	8.57	
28881	G > A	203	R>K	ORF9	3113	4	0.18	0.13	0.73	
28882	G > A	203	R>K	ORF9	3113	4	0.18	0.13	0.73	
28883	G > C	204	G>R	ORF9	3103	4	0.18	0.13	0.73	

423

424

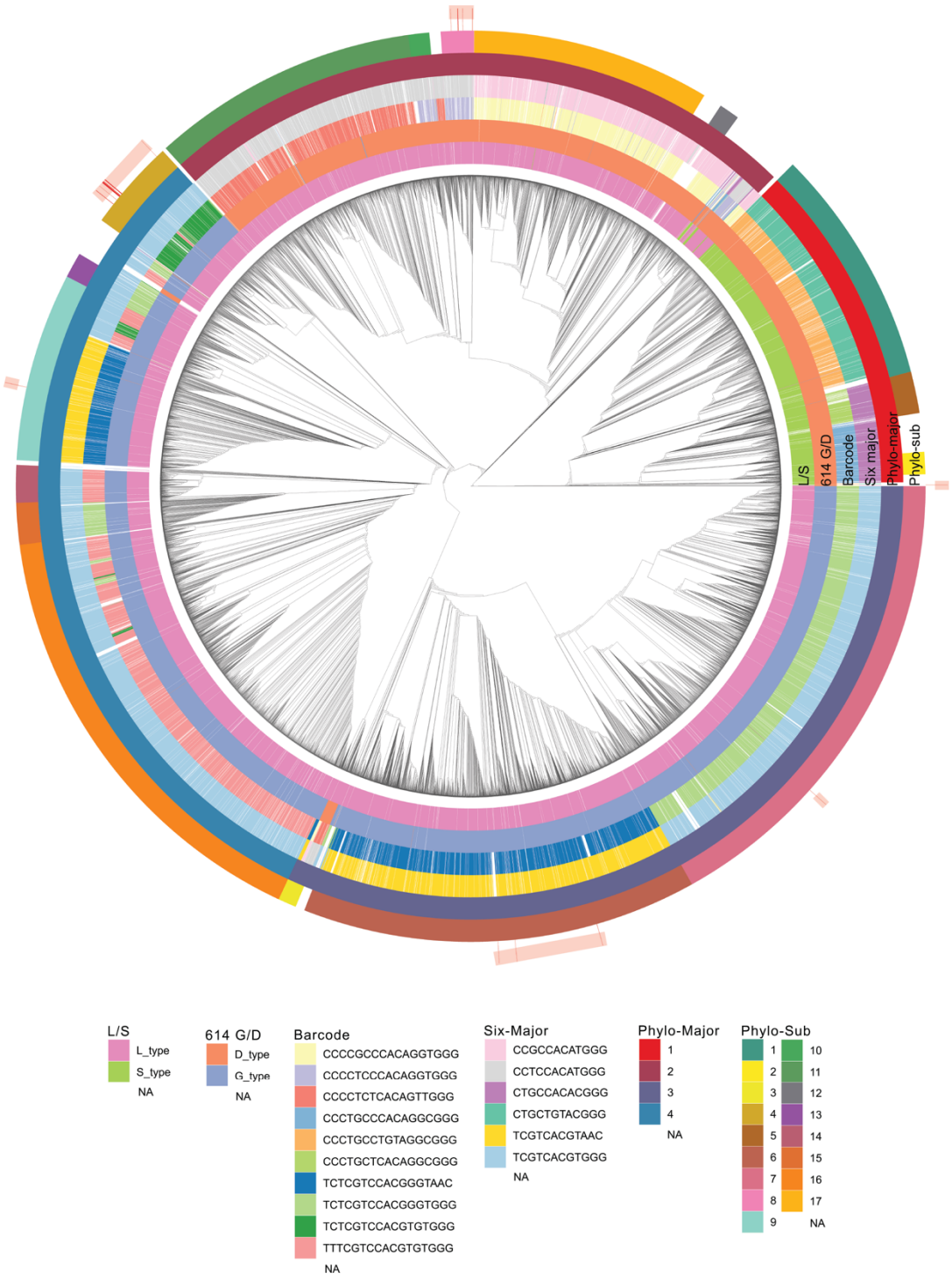

425

426 **Figure 1 - Phylogenetic tree of the 15,277 genomes retrieved from GISAID and their**

427 **groupings.** The time-resolved tree of SARS-CoV-2 appears in the center. Six clustering

428 methods were used to assign15277 sequences to the clusters. The clusters are represented

as circular layers around the tree. The innermost shell (L/S) represents S and L type according to 8782th and 28144th positions in the nucleotide. 614 G/D represents the 614th amino acid of the Spike protein. Barcode shows the 10 major subtypes of seventeen positions in (nucleotide) multiple sequence alignment. Six-major clustering is based on 6 major subtypes of nucleotide combinations in particular positions. The fifth and sixth layers show Phylo-majors and sub-clusters, respectively. Samples obtained from Turkey are shown in the outermost shell and they are highlighted.

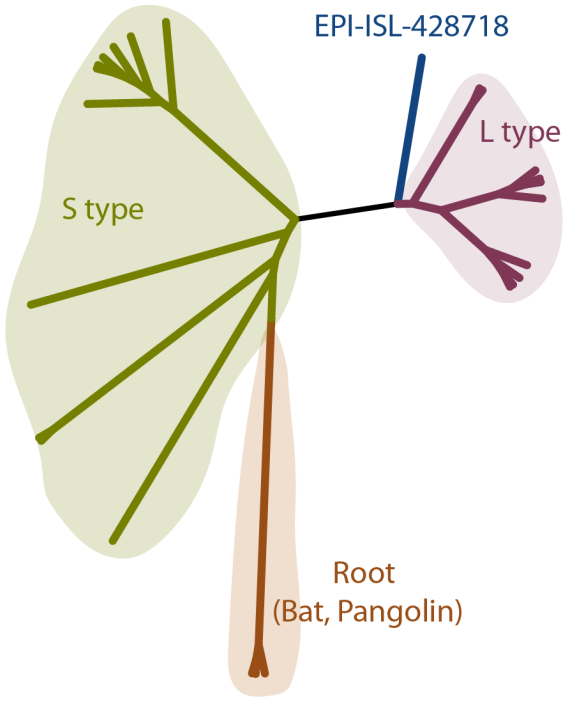

Figure 2 - Phylogenetic tree of the transient type (EPI-ISL-428718) from S to L strain. The maximum likelihood tree was built with IQ-TREE. 10 S-type and 10 L-type sequences are randomly selected from the assigned samples. The tree was rooted at the root of the virus genomes obtained from bat and pangolin.

Figure 3 - Cluster distribution and sub-cluster divergence. (A) Percentages of four major and unknown clusters across different countries. Unknown (U) samples are the ones that cannot be grouped with the generated clusters. (B) Distance distributions of four phylo-sub clusters (4,6,7,8 and 9) found in Turkey, across different countries. The y axis shows log10-scaled root to tip distances.

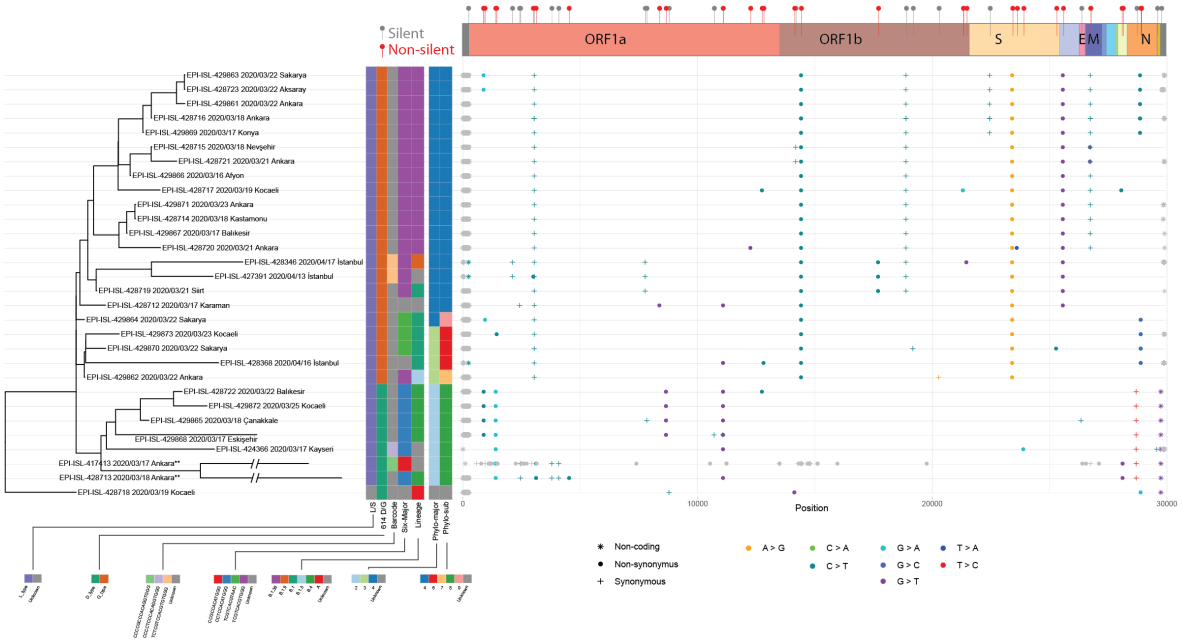

Figure 4 - The mutation layout of the 30 samples from Turkey along with the phylogenetic tree and clusters. Phylogenetic tree (left) of SARS-CoV-2 samples sequenced in Turkey. Assigned subtypes of six clustering methods are specified with different colors in the matrix. Dot-plot (Right) of mutations detected in each genome aligned with the corresponding sample. Single nucleotide changes are colored and shaped based on the nucleotide change and synonymy. Gray color indicates that the mutation is either non-informative (ie, due to sequencing errors) or corresponds to a gap . Supplementary bar (top) provides the respective open reading frame information for mutations, and its effect on coding the amino acid. EPI-ISL-417413 had obviouse sequencing errors, the mutations of this sampled were manually curated and non-informative ones were treated as ambigious mutations.

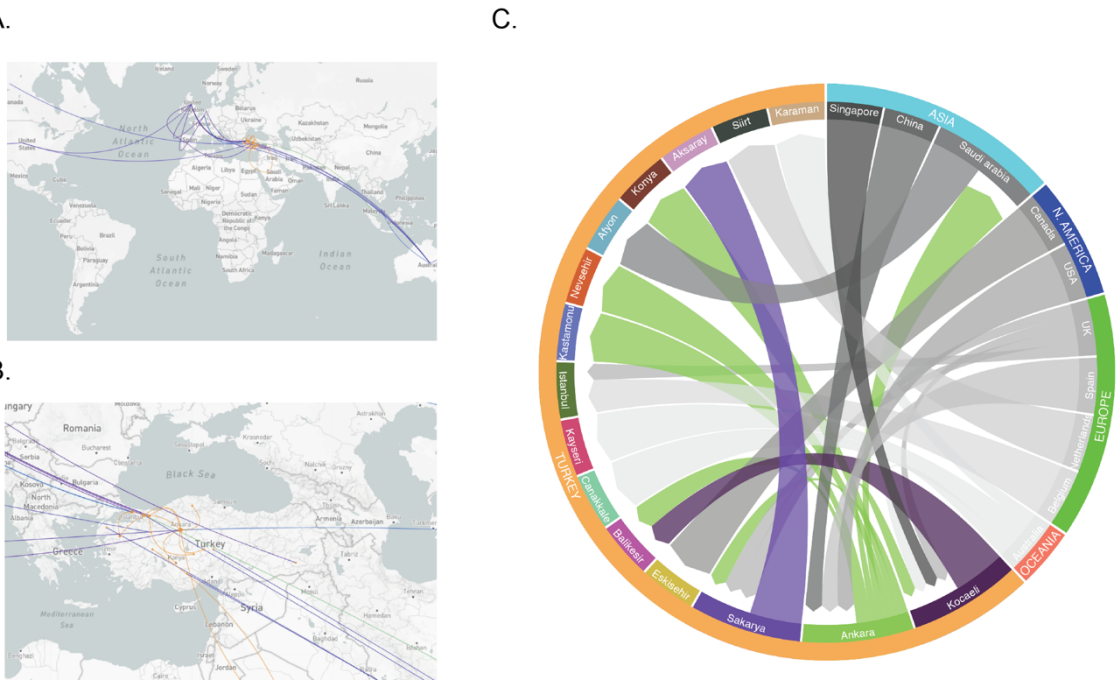

Figure 5 - Epidemiological phylogenetic and transmission analysis of the isolates collected in Turkey. Sequences sampled between 2019-03-19 and 2020-04-24 were analyzed with Treetime and tracing between samples visualized in Augur version 6.4.3. (A) Closest (without internal nodes) members filtered and assigned as transmissions were visualized on Leaflet world map using latitude & longitude information of locations. (B) Samples originated from Turkey were implied with orange points and connections while the network of samples originated from other countries demonstrated with blue lines and points. (C) Chord diagram was used as a graphical method to display inter-flow associations between origins and destinations of transmission data.